J Intell Robot Syst (2007) 50:163–180
DOI 10.1007/s10846-007-9159-4

Performance Analysis and Application of a Redundantly Actuated Parallel Manipulator for Milling

Jun Wu · Jinsong Wang · Tiemin Li · Liping Wang

Received: 13 December 2006 / Accepted: 6 May 2007 /
Published online: 5 June 2007

Abstract This paper deals with the performance analysis of a 3-degree-of-freedom (3-DOF) planar parallel manipulator with actuation redundancy. Closed-form solutions are developed for both the inverse and direct kinematics about the redundant parallel manipulator. In performance analysis phase, the dexterity is analyzed, three kinds of singularities are investigated, and the stiffness is estimated. Compared with the corresponding non-redundant parallel manipulator with the redundant link removed, the redundantly actuated one has better dexterity, litter singular configurations and higher stiffness. The redundantly actuated parallel manipulator was applied to the design of a 4-DOF hybrid machine tool which also includes a feed worktable to demonstrate its applicability.

Keywords Parallel manipulator · Actuation redundancy · Hybrid machine tool

1 Introduction

In some applications where high structural stiffness, position accuracy and dynamic performance are predominant requirements, parallel manipulators offer obvious advantages over serial ones. In the past, most researchers focused on the research of the normally actuated parallel manipulator. However, these manipulators have smaller workspace, lower dexterity and more singular configurations [1–4]. Moreover, singularities lead to a loss of the controllability and degradation of the natural stiffness of manipulators. Thus, singularities make the limited workspace of the manipulators even smaller. Therefore, those potential advantages of parallel manipulators can not be fully realized. In order to profit from the advantages of parallel manipulators, their disadvantages have to be overcome. Redundancy [5, 6] is a solution, which is an effective mean for eliminating or reduce singularities and improving the stiffness of parallel manipulators.

J. Wu (✉) · J. Wang · T. Li · L. Wang
Institute of Manufacturing Engineering, Department of Precision Instruments and Mechanology,
Tsinghua University, Beijing 100084, China
e-mail: wu-j03@mails.tsinghua.edu.cn

Redundancy can be classified into different types [7]. Usually, it is mainly divided into kinematic redundancy and actuation redundancy [8–10]. A manipulator is called kinematically redundant if it possesses more DOF than that is necessary for performing a specified task. Alternatively, a manipulator with actuation redundancy has more joint actuators than that are required to provide the desired end-effector motion. It is noted that actuation redundancy does not affect the mobility of a parallel manipulator and only increases the number of actuators. However, kinematic redundancy involves the introduction of additional DOF and affects the mobility. The kinematical redundant manipulators have been extensively studied, whereas only recently have the parallel manipulators with actuation redundancy drawn attentions.

Actuation redundancy can be introduced to parallel manipulators to eliminate or reduce singularities within the workspace, increase the structure stiffness and improve the dexterity [11, 12]. In addition, using redundant actuation allows for a significant improvement in the force capabilities of parallel manipulators [13]. There are already several applications of parallel mechanisms with actuation redundancy. Kock and Schumacher [14] proposed a redundantly actuated parallel manipulator for high-speed and active-stiffness applications. Kim [15] added two redundant actuators to their eclipse mechanism to eliminate the singularities within the workspace. Cheng et al. [16] built a 2-DOF redundantly actuated parallel manipulator.

In this paper, a planar 3-DOF parallel manipulator with actuation redundancy is proposed. Closed-form solutions are developed for both the inverse and direct kinematics. Based on the kinematics, the dexterity, singularity and stiffness of the redundantly actuated parallel manipulator are investigated. The comparing results with the corresponding non-redundant manipulator with the redundant link removed are given. Combining the redundant parallel manipulator with a feed worktable, a 4-DOF hybrid machine tool is developed to mill metal workpieces. The machining test shows that the hybrid machine tool is suitable for the manufacturing industry.

2 Description of the Parallel Manipulator

The redundant parallel manipulator is shown in Fig. 1 and consists of two sliders, two constant-length links, two extendible links and the moving platform. Sliders are driven by two servomotors fixed on the columns. The kinematic model is shown in Fig. 2. Link A_1B_1 is a redundant link. Sliders A_1A_2 and A_3A_4 drive links A_2B_2 and A_3B_3 when they slide along the vertical guide ways. Links A_1B_1 and A_4B_4, to be driven by two actuators, are extendible struts with one end joined with sliders A_1A_2 and A_3A_4, and the other connected with the moving platform B_1B_2. The whole construction enables movement of the moving platform in a plane and its rotation about the axis normal to the motion plane of the manipulator. The manipulator is redundantly actuated because it has four actuators and only a 3-DOF output.

3 Kinematics Analysis

3.1 Inverse Kinematics

As illustrated in Fig. 2, a base coordinate system *O*-*xyz* is fixed to the base, the *y*-axis is along the beam, the *z*-axis is vertical, and the *x*-axis is normal to the manipulator plane. A

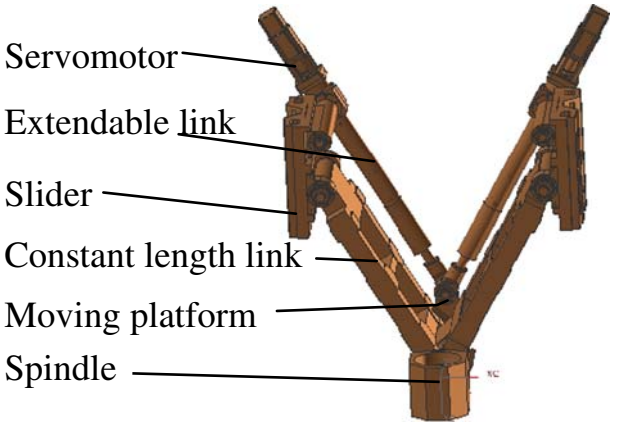

Fig. 1 3D model of the redundant manipulator

moving coordinate system O'-$x'y'z'$ is attached to the moving platform with the z'-axis along the moving platform. Let α be the rotation angle from O'-$x'y'z'$ to O-xyz, and $r_{ai}(i=1, 2, 3, 4)$ and r_{bi} be the position vectors of the joint points A_i and B_i, respectively. Let $\theta_j(j=1, 2, 3, 4)$ be the angles between link A_jB_j and the vertical axis parallel to the z-axis, and $0\leq\theta_1$, $\theta_2\leq\pi$, $-\pi\leq\theta_3$, $\theta_4\leq 0$.

For convenience, the x coordinates of all joint points are assumed to be zero. Then the position vector of the origin O' with respect to O-xyz can be defined as $r_{O'} = [0 \quad y \quad z]^T$.

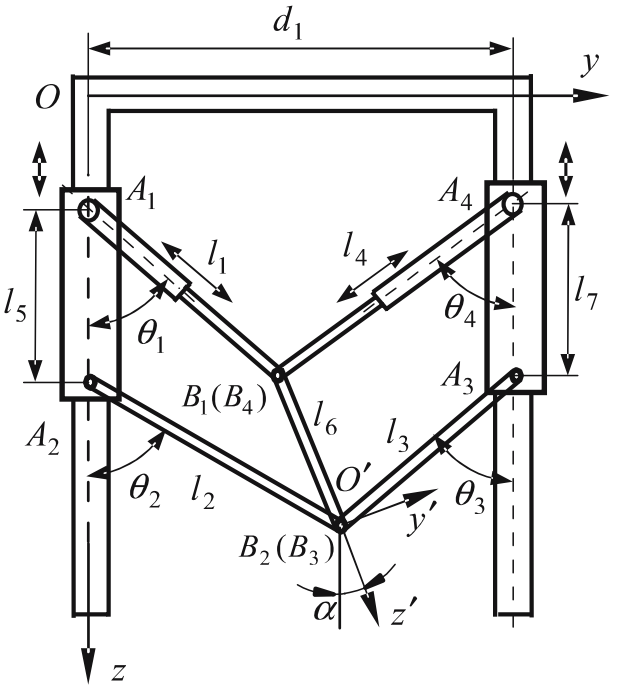

Fig. 2 Kinematic model of the manipulator

The position vectors of joint points B_i with respect to O'-$x'y'z'$ are $r'_{b1} = r'_{b4} = [\,0 \quad 0 \quad -l_6\,]^T$ and $r'_{b2} = r'_{b3} = [\,0 \quad 0 \quad 0\,]^T$, respectively.

The position vector of point B_i in the base coordinate system O-xyz can be then expressed as

$$r_{bi} = r_{O'} + Rr'_{bi} \tag{1}$$

where R is the rotation matrix and can be expressed as

$$R = \begin{bmatrix} 1 & 0 & 0 \\ 0 & \cos\alpha & -\sin\alpha \\ 0 & \sin\alpha & \cos\alpha \end{bmatrix}$$

The position vectors of joint points A_i with respect to O-xyz are

$$r_{a1} = [\,0 \quad 0 \quad z_1\,]^T, r_{a2} = [\,0 \quad 0 \quad z_1 + l_5\,]^T \tag{2}$$

$$r_{a3} = [\,0 \quad d_1 \quad z_4 + l_7\,]^T, r_{a4} = [\,0 \quad d_1 \quad z_4\,]^T \tag{3}$$

where l_6 is the length of the moving platform, d_1 is the width between two columns, l_5 and l_7 are the heights of two sliders, respectively, and z_1 and z_4 are the z coordinates of sliders A_1A_2 and A_3A_4, respectively.

Thus the constraint equation associated with the ith kinematic chain can be written as

$$r_{ai} - r_{bi} = l_i n_i,\ i = 1, 2, 3, 4 \tag{4}$$

where l_i and n_i denote the length and the unit vector of the ith link, respectively.

By taking the 2-norm of both sides of Eq. 4, the following inverse kinematic equations can be obtained

$$z_1 = z - l_5 \pm \sqrt{l_2^2 - y^2} \tag{5a}$$

$$z_4 = z - l_7 \pm \sqrt{l_3^2 - (y - d_1)^2} \tag{5b}$$

$$l_1 = \sqrt{(y - l_6\sin\alpha)^2 + (z - l_6\cos\alpha - z_1)^2} \tag{5c}$$

$$l_4 = \sqrt{(y - l_6\sin\alpha - d_1)^2 + (z - l_6\cos\alpha - z_4)^2} \tag{5d}$$

In practical application, the sliding limits of the sliders can be denoted as $z_1 < z$ and $z_4 < z$ such that the "±" in Eqs. 5a and 5b should be only "–".

It can be seen that the solution of the inverse kinematics is not unique. The number of inverse kinematic solutions of the mechanism is the same as that of its corresponding non-redundant one.

3.2 Direct Kinematics

For the configuration shown in Fig. 2, according to Eq. 4, the solution for the direct kinematics can be expressed as

$$y = l_2 \sin\left[\pi - (\pi/2 + \phi_1 + \phi_2)\right] \tag{6-a}$$

$$z = z_2 + l_2 \cos\left[\pi - (\pi/2 + \phi_1 + \phi_2)\right] \tag{6-b}$$

$$\alpha = \beta_1 - \beta_2 \tag{6-c}$$

where $\phi_1 = \arccos\frac{l_2^2+d_1^2+(z_3-z_2)^2-l_3^2}{2l_2\sqrt{d_1^2+(z_3-z_2)^2}}$,

z_2 and z_3 are the z coordinates of joint points A_2 and A_3, and z_3=z_4+l_7,

$$\phi_2 = \arctan\left[(z_3 - z_2)/d_1\right], \theta_3 = \arcsin\left[(d_1 - y)/l_3\right]$$

$$l_8 = \|A_4B_2\| = \sqrt{l_3^2 + l_7^2 + 2l_3l_7\cos\theta_3},$$

$$\beta_1 = \arccos\left(\frac{l_6^2 + l_8^2 - l_4^2}{2l_6l_8}\right), \beta_2 = \arccos\left(\frac{l_7^2 + l_8^2 - l_3^2}{2l_7l_8}\right),$$

In fact, as shown in Fig. 2, the following vector equation can be obtained

$$\vec{z}_1 + \vec{l}_1 + \vec{l}_4 + \vec{z}_4 + \vec{d}_1 = 0 \tag{7}$$

It shows that four input variables z_1, z_4, l_1 and l_4 are interrelated. Moreover, when three of four input variables are given, another input variable can be uniquely determined.

It is noteworthy that the corresponding non-redundant manipulator with a similar configuration shown in Fig. 2 has two solutions for the direct kinematics. Thus, the redundant parallel manipulator has less number of direct kinematic solutions than its corresponding non-redundant manipulator.

3.3 Jacobian Matrix

Jacobian matrix J of the parallel manipulator, which is a $m\times n$ matrix, is a mapping from the joint velocity vector to the Cartesian velocity vector. Here, m is the number of the actuators, and n is the number of DOF. For a non-redundant parallel manipulator, there is m=n, and m>n for a redundantly actuated manipulator.

Taking the derivative of Eqs. 5a–5d with respect to time leads to

$$\dot{q} = J\dot{p} \tag{8}$$

where $\dot{q} = \begin{bmatrix}\dot{z}_1 & \dot{z}_4 & \dot{l}_1 & \dot{l}_4\end{bmatrix}^T$, $\dot{p} = \begin{bmatrix}\dot{y} & \dot{z} & \dot{\alpha}\end{bmatrix}^T$, and J is the Jacobian matrix and can be written as

$$J = \begin{bmatrix} y/(z-z_2) & 1 & 0 \\ (y-d_1)/(z-z_3) & 1 & 0 \\ J_{31} & 0 & J_{33} \\ J_{41} & 0 & J_{43} \end{bmatrix}$$

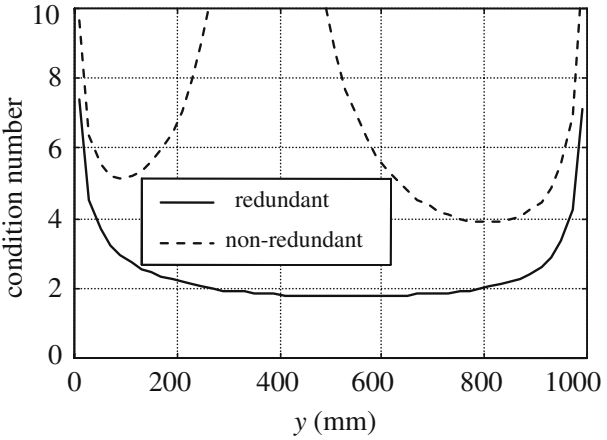

Fig. 3 Condition number on α=-30°

where

$$J_{31} = \frac{y - l_6 \sin\alpha - y(z - l_6 \cos\alpha - z_1)/(z - z_2)}{l_1},$$

$$J_{33} = \frac{(z - z_1) l_6 \sin\alpha - y l_6 \cos\alpha}{l_1},$$

$$J_{41} = \frac{y - l_6 \sin\alpha - d_1}{l_4} - \frac{(z - l_6 \cos\alpha - z_4)(y - d_1)}{l_4 (z - z_3)},$$

$$J_{43} = \frac{(z - z_4) l_6 \sin\alpha - (y - d_1) l_6 \cos\alpha}{l_4}.$$

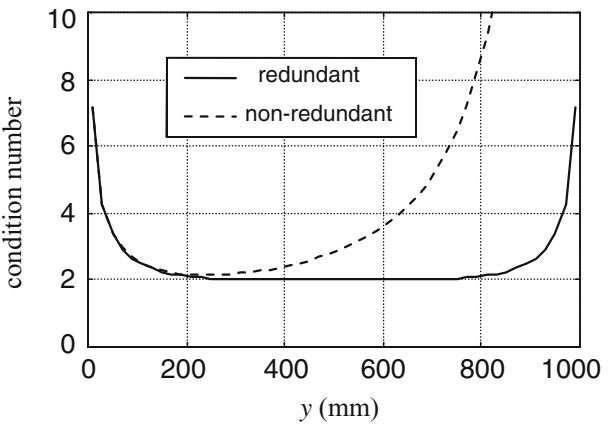

Fig. 4 Condition number on α=0°

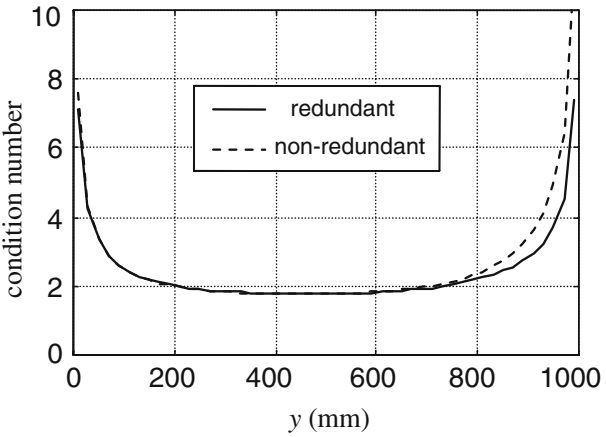

Fig. 5 Condition number on α=30°

4 Performance Analysis of the Redundant Parallel Manipulator

4.1 Dexterity Index

The condition number is regarded as the performance index for evaluating the dexterity [17, 18]. The singular value σ_i of the Jacobian matrix is given by

$$\sigma_i = \sqrt{\lambda_i(JJ^T)}, i = 1, 2, \cdots, n(n \leq m) \tag{9}$$

where $\lambda_i(J^TJ)$ is the eigenvalue of matrix J^TJ.Then the condition number κ can be expressed as

$$1 \leq \kappa = \frac{\sigma_{\max}}{\sigma_{\min}} \leq \infty \tag{10}$$

where $\sigma_{\max}$ and $\sigma_{\min}$ are the maximum and minimum singular values of the Jacobian matrix associated with a given pose.

In a pose where the condition number is equal to 1, the dexterity of the manipulator is best and the manipulator is isotropic. Designing a parallel manipulator that is isotropic in one pose or over its full workspace is often considered as a design objective. When the y coordinate of the moving platform varies from 0 to 1,000 mm and the rotation angle α ranges between −90 and 90°, the condition number of the redundantly actuated parallel manipulator always goes to 2, as shown in Figs. 3, 4, 5. The corresponding non-redundant manipulator is shown in Fig. 6, and the condition number of the non-redundant manipulator is much larger than that of the redundant one. Thus, the redundant parallel manipulator has better isotropy and dexterity in the workspace.

When y=400 and α=−30°, the condition number of the non-redundant manipulator varies so greatly that the maximum value of the condition number beyond the limit of vertical axis, as shown in Fig. 3. The reason is that the non-redundant manipulator nears the direct kinematic singular configuration and the dexterity is very bad. On the contrary, the condition number of the redundant parallel manipulator changes smoothly for the singular configuration being overcome.

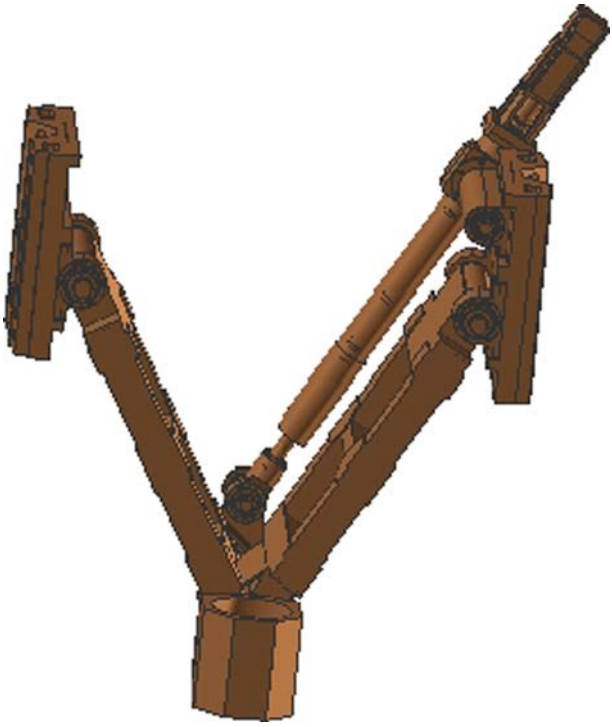

Fig. 6 3D model of non-redundant manipulator

4.2 Singularity Analysis

From the viewpoint of differential motion, one or more singular values of J are infinite when the inverse kinematic singularity occurs and infinitesimal motion of the moving platform along certain directions cannot be accomplished. Considering that $\det\left(J^T J\right) = \prod \sigma_i^2$, the following equation can be obtained

$$\det\left(J^T J\right) = \infty \tag{11}$$

When one or more singular values of J are zero, the direct kinematic singularity occurs and the moving platform can possess infinitesimal motion in some directions even if all the actuators are completely locked. By taking $\det\left(J^T J\right) = \prod \sigma_i^2$ into account, it has

$$\det\left(J^T J\right) = 0 \tag{12}$$

When the combined singularity exists, it has

$$tr\left(J^T J\right) = \sum_{i=1}^{n} \sigma_i^2 = \infty \tag{13}$$

where $tr\left(J^T J\right)$ is the trace of matrix $J^T J$.

The following will discuss the effect of actuation redundancy on the direct kinematic singularity and take the redundant manipulator studied here as an example to analyze its singularity.

4.2.1 The Effect of Actuation Redundancy on Direct Kinematic Singularity

Equation 8 can be rewritten as

$$\begin{bmatrix} \dot{q}_{\mathrm{u}} \\ \dot{q}_{\mathrm{r}} \end{bmatrix} = \begin{bmatrix} J_{\mathrm{u}} \\ J_{\mathrm{r}} \end{bmatrix} \dot{P} \tag{14}$$

where J_{u} is the Jacobian matrix of the corresponding non-redundant manipulator, J_{r} is the Jacobian matrix of the redundant links, and $\dot{q_u}$ and $\dot{q_r}$ are the active joint velocities of the non-redundant manipulator and the redundant links, respectively.

Thus, it can be obtained that

$$\det\left(J^T J\right) = \det\left(J_u^T J_u + J_r^T J_r\right) \tag{15}$$

Since $J_u^T J_u$ and $J_r^T J_r$ are semi-positive matrices, two orthogonal basis $Q_u = [\, q_1^u \quad \cdots \quad q_n^u \,]$ and $Q_{\mathrm{r}} = \left[\, q_{n+1}^u \quad \cdots \quad q_m^u \,\right]$ can be found to satisfy

$$Q_u^T J_u^T J_u Q_u = diag\left(\lambda_1^u, \lambda_2^u, \cdots, \lambda_n^u\right) \tag{16}$$

$$Q_r^T J_r^T J_r Q_r = diag\left(\lambda_{n+1}^r, \lambda_{n+2}^r, \cdots, \lambda_m^r\right) \tag{17}$$

where λ_n^u and λ_m^r are the eigenvalues of $J_u^T J_u$ and $J_r^T J_r$, respectively, and $\lambda_1^u \geq \lambda_2^u \cdots \geq \lambda_n^u$.

When the non-redundant parallel manipulator experiences a direct kinematic singularity, there is at least one eigenvalue of $J_u^T J_u$ being 0 and can be expressed as

$$\lambda_i^u = \lambda_{i+1}^u = \cdots = \lambda_n^u = 0 \tag{18}$$

where λ_i^u is the ith eigenvalue being 0.

Accordingly,

$$J_u q_i^u = 0 \tag{19}$$

When the redundant parallel manipulator experiences a direct kinematic singularity, it has $\det\left(J_u^T J_u + J_r^T J_r\right) = 0$ and the following equation can be obtained

$$X^T \left(J_u^T J_u + J_r^T J_r\right) X = 0 \tag{20}$$

where X is n-dimension matrix and $X \in span\left\{q_1^u, \cdots, q_n^u\right\}$.

Since $J_u^T J_u$ and $J_r^T J_r$ are semi-positive, it has

$$X^T J_u^T J_u X = 0 \tag{21}$$

$$X^T J_r^T J_r X = 0 \tag{22}$$

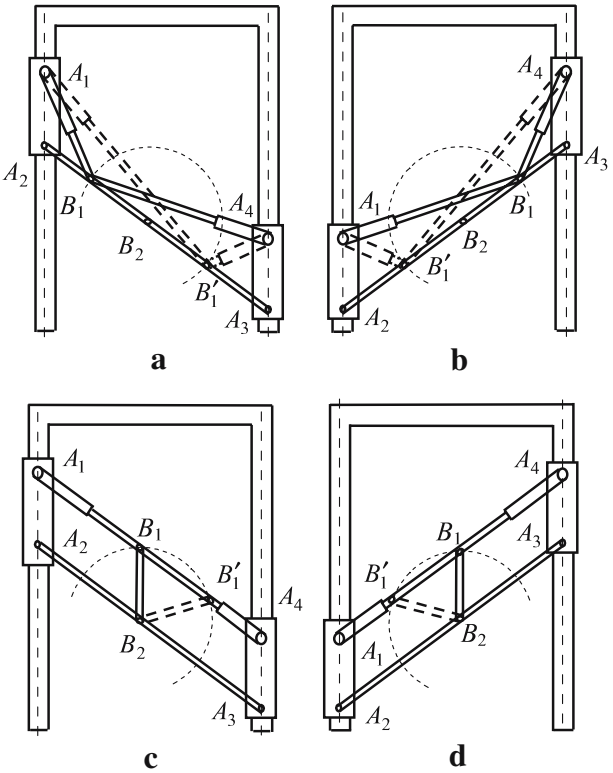

Fig. 7 Direct kinematic singularity. **a** $\alpha=\theta_2$ and the configuration $A_1B_1'A_4$ corresponds to $\alpha=\theta_3$, **b** $\alpha=\theta_3$ and the configuration $A_1B_1'A_4$ corresponds to $\alpha=\theta_2$, **c** and **d** the four singular configurations correspond to $\theta_2-\theta_3=\pi$ and $\theta_1-\theta_4=\pi$

According to Eq. 21, X is determined by

$$X = c_i q_i^u + c_{i+1} q_{i+1}^u + \cdots + c_n q_n^u \tag{23}$$

where $c_i,...c_n$ are the coefficient.

Based on Eqs. 22 and 23, it can be concluded that

$$\sum_{i=1}^{n} c_i^2 \left(q_i^u\right)^T J_r^T J_r q_i^u = 0 \tag{24}$$

Namely,

$$J_r\, q_i^u = 0 \cdot q_i^u \tag{25}$$

From Eqs. 19 and 25, it can be seen that the eigenvector that the 0 eigenvalue of J_u corresponds is also the eigenvector that 0 eigenvalue of J_r corresponds. As long as the eigenvector that the 0 eigenvalue of J_u corresponds does not include the eigenvector that 0 eigenvalue of J_r corresponds, the direct kinematic singularity can not occur.

Thus, in order to overcome all direct kinematic singularities in the workspace, the motion direction of actuation redundancy should not be parallel to the eigenvector that the 0 eigenvalue of J_u corresponds.

Thus, actuation redundancy mainly eliminates the direct kinematic singularity and accordingly reduces the combined singularity.

4.2.2 Singularity of the Redundant Parallel Manipulator

From Eq. 8, it can be concluded that

$$\det\left(J^T J\right) = \left(J_{33}^2 + J_{43}^2\right)(J_{11} - J_{21})^2 + 2(J_{33}J_{41} - J_{31}J_{43})^2 \tag{26}$$

where $J_{11} = y/(z - z_2)$, $J_{21} = (y - d_1)/(z - z_3)$.

1. Direct kinematic singularity.

This kind of singularity occurs when $\det(J^T J) = 0$. Namely, either of the following two equations is satisfied

$$\begin{cases} J_{11} = J_{21} \\ J_{33}J_{41} = J_{31}J_{43} \end{cases} \tag{27}$$

$$J_{33} = J_{43} = 0 \tag{28}$$

For convenience, J_{31}, J_{33}, J_{41} and J_{43} can be rewritten as

$$J_{31} = \frac{\sin(\theta_1 - \theta_2)}{\cos\theta_2}, J_{33} = l_6 \sin(\alpha - \theta_1) \tag{29}$$

$$J_{41} = \frac{\sin(\theta_4 - \theta_3)}{\cos\theta_3}, J_{43} = l_6 \sin(\alpha - \theta_4) \tag{30}$$

(a) Equation 27 is satisfied. On one hand, the equation J_{11}=J_{21} can be rewritten as

$$\frac{y}{z - z_2} = \frac{y - d_1}{z - z_3} \tag{31}$$

It shows that joint points A_2, B_2 and A_3 are collinear which result in $\theta_2-\theta_3=\pi$.

On the other hand, $J_{33}J_{41}$=$J_{31}J_{43}$ can be rewritten as

$$\frac{\sin(\theta_2 - \theta_1)}{\sin(\theta_2 - \theta_4)} = \frac{\sin(a - \theta_1)}{\sin(\alpha - \theta_4)} \tag{32}$$

Taking the limit of θ_i (i=1, 2, 3, 4) into account, the possible solutions of Eqs. 31 and 32 can be written as: (1) $\theta_2-\theta_3=\pi$, $\alpha=\theta_2$; (2) $\theta_2-\theta_3=\pi$, $\alpha=\theta_3$; and (3) $\theta_2-\theta_3=\pi$, $\theta_1-\theta_4=\pi$. The three solutions correspond to eight singular configurations shown in Fig. 7. In Fig. 7a, $\alpha=\theta_2$ and the configuration $A_1B_1^{'}A_4$ corresponds to $\alpha=\theta_3$; In Fig. 7b, $\alpha=\theta_3$ and the configuration $A_1B_1^{'}A_4$ corresponds to $\alpha=\theta_2$. In Fig. 7c and d, the four singular configurations correspond to $\theta_2-\theta_3=\pi$ and $\theta_1-\theta_4=\pi$.

When the redundant manipulator is in a singular configuration, not only joint points A_2, B_2 and A_3 are collinear, but also the orientation of the moving platform must be in one of eight possible orientations.

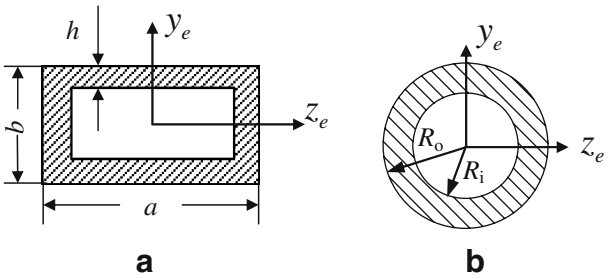

Fig. 8 Cross-sections of links. **a** Constant length link and **b** extendible link

(b) Equation 28 is satisfied. Equation J_{33}=J_{43}=0 can be rewritten as

$$\begin{bmatrix} z-z_1 & -y \\ z-z_4 & -y+d_1 \end{bmatrix} \begin{bmatrix} \sin\alpha \\ \cos\alpha \end{bmatrix} = 0 \tag{33}$$

Since $[\sin\alpha \quad \cos\alpha]^T \neq 0$, the following equation can be obtained

$$\begin{vmatrix} z-z_1 & -y \\ z-z_4 & -y+d_1 \end{vmatrix} = 0 \tag{34}$$

It means that points A_1, B_2 and A_4 are collinear. Due to the mechanism limit, the redundant manipulator studied here can not reach this configuration.

When joint points A_2, B_2 and A_3 are collinear, the corresponding non-redundant parallel manipulator with its moving platform at a random orientation experiences a singularity. However, when the redundant manipulator approaches the singular configuration, not only joint points A_2, B_2 and A_3 are collinear, but also the orientation of the moving platform must be in one of the eight possible configurations. In addition, the non-redundant parallel manipulator reaches the singular configuration when the moving platform B_1B_2 and link A_4B_4 are in the same line. Thus, the singular configurations of the redundant manipulator are reduced significantly relative to the non-redundant one.

2. Inverse kinematic singularity.

This kind of singularity occurs when $\det(J^TJ) = \infty$. Namely, either of the following two equations is satisfied

$$z = z_2 \neq z_3 \tag{35}$$

$$z = z_3 \neq z_2 \tag{36}$$

At this time, one of links A_2B_2 or A_3B_3 is horizontal. Under this condition, the redundant manipulator has the same singular configurations as its corresponding non-redundant one.

3. Combined singularity.

This kind of singularity occurs when both direct kinematic singularities and inverse kinematic singularities exist simultaneously. It is not only configuration-dependent, but also architecture- dependent. In this case, l_2+l_3=d_1. For the redundant manipulator discussed here, it is impossible to reach this configuration due to the architecture limitation of the manipulator. However, combined singularity will occur in the non-redundant manipulator.

From above analysis, it can be concluded that the singular configurations of the redundant parallel manipulator are reduced significantly in comparison with those of the corresponding non-redundant manipulator.

Table 1 Parameters of cross-sections of legs (mm)

Constant length leg		Extendable leg		
a	500		R_i	R_o
b	100	Upper part	0	19
h	10	Lower part	20	30

4.3 Stiffness Analysis

4.3.1 Stiffness Modeling

Stiffness is one of the most important performance specifications of parallel manipulators [19, 20]. In stiffness modeling, the machine structure can be decomposed into two substructures, the machine frame and the parallel link substructure [21]. The stiffness model of each substructure is formulated by assuming that the components in the other are rigid. Then the stiffness of the parallel manipulator can be achieved by linear superposition of the two substructures.

In practice, the stiffness of machine frame is much higher than that of the parallel link. Therefore, the machine frame is assumed to be rigid and the stiffness of parallel link is regarded as the stiffness of the parallel manipulator. The basic assumptions for stiffness modeling are given as follows:

1. The joints are frictionless and their deformation is negligible.
2. The rigidities of the moving platform and the machine frame are much higher than those of the other components and can be considered as infinite.

Under the wrench $\begin{bmatrix} F^T & M^T \end{bmatrix}^T$ applied on the moving platform, the axial stiffness of links will cause the platform to undergo a twist $\begin{bmatrix} \Delta_p^T & \Theta_p^T \end{bmatrix}^T$. Thus, virtual work principle has the form

$$\begin{bmatrix} \delta\Delta_p^T & \delta & \Theta_p^T \end{bmatrix} \begin{bmatrix} F \\ M \end{bmatrix} = \sum_{i=1}^{4} \delta\Delta L_i n_i^T f_i \tag{37}$$

where ΔL_i and f_i are the deformation and axial force of the ith (i=1, 2, 3, 4) link, and $f_i = k_{pi}\Delta L_i n_i$. Here

$$\frac{1}{k_{pi}} = \frac{1}{k_{i1}} + \frac{2}{k_{i2}} \tag{38}$$

where k_{i1} and k_{i2} are the stiffness of the ith link and the joint, respectively. For the extendible link, the upper and lower parts are connected in series. Then

$$\frac{1}{k_{i1}} = \frac{1}{k_{iu}} + \frac{1}{k_{ib}}, i = 1, 4 \tag{39}$$

Table 2 Geometric parameters of the redundant manipulator (mm)

Parameters	l_2	l_3	l_5	l_6	l_7	d_1
Values	1,000	1,000	300	300	300	1000

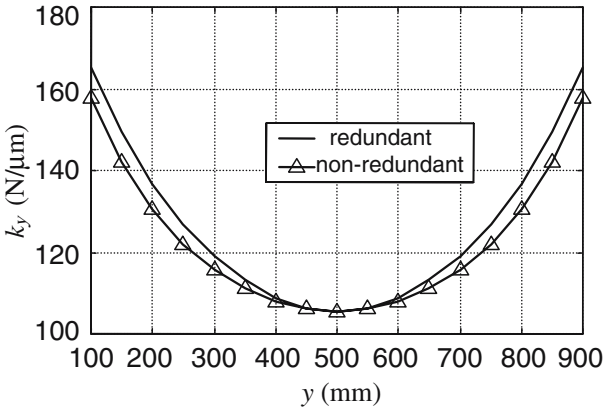

Fig. 9 y direction stiffness distribution

where k_{iu}, k_{ib} are the stiffness of the upper and the lower parts of the extendible leg, respectively.

Then Eq. 37 can be rewritten as

$$\begin{bmatrix} \delta\Delta_p^T & \delta\Theta_p^T \end{bmatrix} \begin{bmatrix} F \\ M \end{bmatrix} = \delta\Delta L^T K_{\mathrm{p}} \Delta L \tag{40}$$

where

$$\Delta L = [\, \Delta L_1 \quad \Delta L_2 \quad \Delta L_3 \quad \Delta L_4 \,]^T,$$

$$K_p = diag\left(k_{p1}, k_{p2}, k_{p3}, k_{p4}\right).$$

Equation 4 can be rewritten as

$$r_{O'} + r'_{bi} = r_{ai} + l_i n_i \tag{41}$$

Small perturbation on both sides of Eq. 41 and implementing linearization yields

$$\Delta_p + \Theta_p \times r'_{bi} = \Delta L_i n_i + L_i \varphi_i \times n_i \tag{42}$$

where φ_{i} is the angle deformation of ith link.

Multiplying both sides of Eq. 42 by n_i^T leads to

$$\Delta L_i = \begin{bmatrix} n_i^T & \left(r'_{\mathrm{bi}} \times n_{\mathrm{i}}\right)^T \end{bmatrix} \begin{bmatrix} \Delta_p \\ \Theta_p \end{bmatrix} \tag{43}$$

Equation 43 can be rearranged in matrix form as

$$\Delta L = J_{\mathrm{p}} \begin{bmatrix} \Delta_p \\ \Theta_p \end{bmatrix} \tag{44}$$

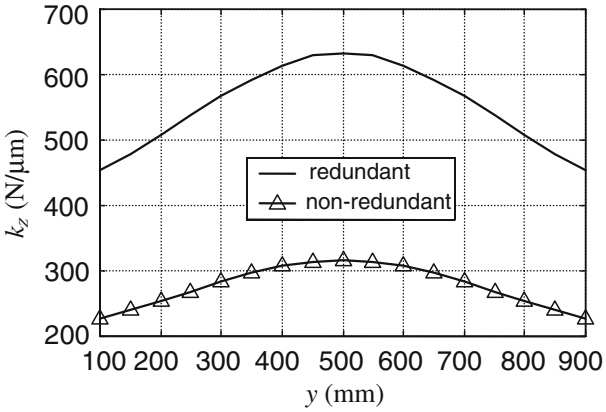

Fig. 10 z direction stiffness distribution

where

$$J_{\mathrm{p}} = \begin{bmatrix} n_1 & n_2 & n_3 & n_4 \\ r'_{\mathrm{b1}} \times n_1 & r'_{\mathrm{b2}} \times n_2 & r'_{\mathrm{b3}} \times n_3 & r'_{\mathrm{b4}} \times n_4 \end{bmatrix}^T$$

Substituting Eq. 44 into 40 results in the stiffness model of the parallel link substructure as

$$\begin{bmatrix} F \\ M \end{bmatrix} = K \begin{bmatrix} \Delta_p \\ \Theta_p \end{bmatrix} \tag{45}$$

where $K = J_p^T K_p J_p$. k_{y} and k_z are defined as the stiffness distributions of the manipulator in y and z directions, and k_α denotes the rotational stiffness distribution about the x-axis. The

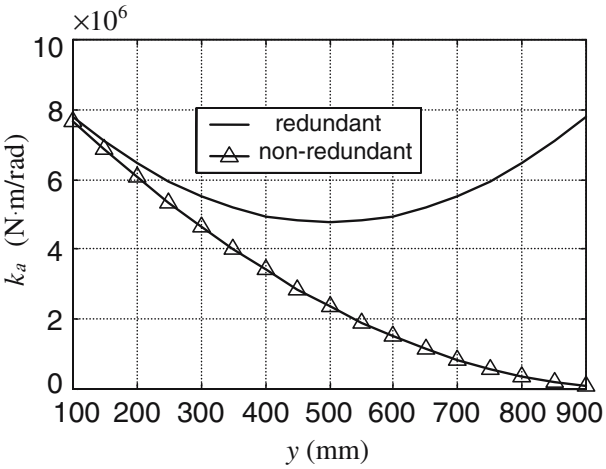

Fig. 11 x direction rotation stiffness

Fig. 12 Prototype of the hybrid machine tool

stiffness matrix of the redundant manipulator can be achieved by deleting the column and row with all elements being zeros of K.

4.3.2 Simulation Results of Stiffness

The cross-section parameters of the links are shown in Fig. 8 and Table 1, and the geometrical parameters of the redundant parallel manipulator are listed in the Table 2. The coordinate of the moving platform is $y \in [0, 1{,}000]$ mm and $\alpha = 0$. All joint stiffness is 5.09×10^8 N/m, and the Young's modulus of links are all 210GPa.

The stiffness distribution in yz plane of the redundant manipulator and that of the corresponding non-redundant manipulator are shown in Figs. 9, 10, 11. It is worth pointing out that the stiffness distribution k_y of the non-redundant manipulator is approximately symmetrical about $y = \frac{d_1}{2}$. The reason is that the tool is fixed on the end point B_2 of the moving platform and k_y is the stiffness of point B_2. If the tool is fixed on the midpoint of the moving platform B_1B_2, k_y on the midpoint of platform B_1B_2 will not be symmetrical about $y = \frac{d_1}{2}$ and monotonously descending in the y direction.

It can be seen that the stiffness distribution of y direction of the redundant manipulator is higher than that of its corresponding non-redundant manipulator. The z direction position stiffness and the rotation stiffness about the x-axis of the redundant manipulator are much higher than those of the non-redundant one. Moreover, the stiffness distribution k_a of the redundant manipulator is approximately symmetrical about $y = d_1/2$. Hence, the stiffness

Fig. 13 Test of machining

of the redundantly actuated manipulator is larger than that of the non-redundant manipulator. The stiffness performance of the redundant manipulator has been improved.

5 Application

By combining the redundantly actuated parallel manipulator with a feed worktable, a 4-DOF hybrid machine tool was created, as shown in Fig. 12. The machine tool is manufactured by Tsinghua University. Figure 13 is the photo of the test to machine a metal workpiece with a large depth of cut, and the result of the test shows that the machine tool can run stably in the machining process.

6 Conclusions

The performance analysis and application of a planar 3-DOF parallel manipulator with actuation redundancy have been investigated in this article. From this investigation, the following conclusions can be drawn:

1. Compared to the corresponding non-redundant parallel manipulator, the 3-DOF redundant parallel manipulator has the same number of inverse kinematic solutions and less number of direct kinematic solutions.
2. The 3-DOF parallel manipulator with actuation redundancy has better dexterity, litter singular configuration and higher stiffness than its corresponding non-redundant one with the redundant link removed.
3. The proposed redundant parallel manipulator has been employed for the development of a hybrid machine tool for the manufacturing industry.

Acknowledgements This work is supported by the National Nature Science Foundation of China (grant no.50605041 and 50505023), the Scientific and Technical Essential Program (grant no. 2006BAF01B09), the 863 High-Tech Scheme (grant no. 2004AA424120 and 2005AA424220) and the "973" key fundamental programs of China (grant no. 2004CB318007 and 2006CB705400).

The authors gratefully acknowledge the discussion on the paper with Professor Xin-Jun Liu.

References

1. Li, Y., Xu, Q.: A new approach to the architecture optimization of a general 3-PUU translational parallel manipulator. J. Intell. Robot. Syst. Theory Appl. **46**(1), 59–72 (2006)
2. Guenter, P.: Parallel kinematic machines (PKM)–limitations and new solutions. CIRP Annals-Manufacturing Technology **49**(1), 275–280 (2000)
3. Merlet, J.P.: Redundant parallel manipulators. Lab. Robot. Autom. **8**(1), 17–24 (1996)
4. Wu, J., Wang, J., Li, T., Wang, L.: Analysis and application of a 2-DOF planar parallel mechanism. ASME J. Mech. Des. **129**(4), 434–437 (2007)
5. Ropponen, T.: Actuation redundancy in a closed-chain robot mechanism. Ph.D. dissertation, Helsinki University of Technology (1993)
6. Ropponen, T., Nakamura, Y.: Singularity-free parameterization and performance analysis of actuation redundancy. Proc. of IEEE int. conf. on robotics and automation, pp. 806–811 (1990)
7. Conkur, E.S., Buckingham, R.: Clarifying the definition of redundancy as used in robotics. Robotica **15**(5), 583–586 (1997)
8. Wang, J., Gosselin, C.M.: Kinematic analysis and design of kinematically redundant parallel mechanisms. ASME J. Mech. Des. **126**(1), 109–118 (2004)
9. Kim, S.: Operational quality analysis of parallel manipulators with actuation redundancy. Proc. of IEEE int. conf. on robotics and automation, pp. 2651–2656 (1997)
10. Chakarov, D.: Study of the antagonistic stiffness of parallel manipulators with actuation redundancy. Mech. Mach. Theory, **39**(6), 583–601 (2004)
11. Obrien, J.F., Wen, J.T.: Redundant actuation for improving kinematic manipulability. Proc of IEEE int. conf. on robots and automation, pp. 1520–1525 (1999)
12. Cheng, H., Liu, G.F., Xiong, Z.H., Li, Z.X.: Advantages and dynamics of parallel manipulators with redundant actuation. Proc of IEEE/RSJ int. conf. on intelligent robots and systems, pp. 171–176 (2001)
13. Nokleby, S.B., Fisher, R., Podhorodeski, R.P., Firmani, F.: Force capabilities of redundantly actuated parallel manipulators. Mech. Mach. Theory **40**(5), 578–599 (2005)
14. Kock, S., Schumacher, W.: A parallel x–y manipulator with actuation redundancy for high-speed and active-stiffness applications. Proc of IEEE int. conf. on robotics and automation, pp. 2295–2300 (1998)
15. Kim, J., et al.: Design and analysis of a redundantly actuated parallel mechanism for rapid machining. IEEE Trans. Robot Autom. **17**(4), 423–434 (2001)
16. Cheng, H., Yiu, Y.K., Li, Z.X.: Dynamics and control of redundantly actuated parallel manipulators. IEEE/ASME Trans. Mechatron. **8**(4), 483–491 (2003)
17. Carretero, J.A., Podhorodeski, R.P., Nahon, M.A., Gosselin, C.M.: Kinematic analysis and optimization of a new three degree-of-freedom spatial parallel manipulator. ASME J. Mech. Des. **122**(1), 17–24 (2000)
18. Oh, K.-K., Liu, X.-J., Kang, D.S., Kim, J.: Optimal design of a micro-parallel positioning platform. Part I: Kinematic analysis. Robotica **22**(6), 599–609 (2004)
19. Liu, X.-J.: Optimal kinematic design of a three translational DoFs parallel manipulator. Robotica **24**(2), 239–250 (2006)
20. Liu, X.-J., Wang, J., Pritschow, G.: Performance atlases and optimum design of planar 5R symmetrical parallel mechanism. Mech. Mach. Theory, **41**(2), 119–144 (2006)
21. Li, Y.-W, Wang, J.-S., Wang, L.P.: Stiffness analysis of a Stewart platform-based parallel kinematic machine. IEEE Int. Conf. Robot. Autom., pp. 3672–3677 (2002)